

Flow Injection Glutamate Biosensor Based on Carbon Nanotubes and Pt-Nanoparticles Using FFT Continuous Cyclic Voltammetry

P. Norouzi^{1,2,*}, F. Faridbod,² H. Rashedi,³ M. R. Ganjali^{1,2}

¹ Center of Excellence in Electrochemistry, University of Tehran, Tehran, Iran

² Endocrinology and Metabolism Research Center, Tehran University of Medical Sciences, Tehran, Iran

³ Department of Biochemistry Engineering, Faculty of Engineering, University of Tehran, Tehran, Iran

*E-mail: norouzi@khayam.ut.ac.ir

Received: 2 October 2010 / Accepted: 30 October 2010 / Published: 1 December 2010

Glutamate concentration was measured by a novel glutamate dehydrogenase biosensor in a flow injection analysis (FIA) system. The measurement method was based on application of fast Fourier transformation continuous cyclic voltammetry (FFTCCV) in which the current under the glutamate voltammogram integrated (after removing the noise frequencies and background subtraction) in a specific potential range. The biosensor was assembled by modifying glassy carbon electrode surface with multiwall carbon Nanotubes (MWCNTs), Pt nanoparticles (PtNPs) and glutamate dehydrogenase (GD) immobilized by nafion. The combination of nanoparticles catalyzed electron transfer mechanism and amplifying the detection sensitivity. The biosensor characterization was studied by scanning electron microscopy (SEM) and electrical impedance spectroscopy (EIS). Also, experimental parameters affected the sensitivity of the biosensors including potential scan rate, solution flow rate and buffer pH was studied. The calculated charge was proportional to its concentration in the range from 0.1 to 50 μM , with a detection limit of 5 nM. The biosensor showed good reproducibility and long-term storage stability.

Keywords: Pt nanoparticles, glutamate, glutamate dehydrogenase, biosensor, FFT cyclic voltammetry

1. INTRODUCTION

Glutamic acid (non-essential amino acid in human, Fig. 1) is one of the 20 proteinogenic amino acids with GAA and GAG codons. The carboxylate anion and salts of glutamic acid are known as glutamate. The side chain carboxylic acid functional group has pK_a of 4.1, and it exists in negatively

charged deprotonated carboxylate form at physiological pH. Glutamate is a key molecule in cellular metabolism. It is an important neurotransmitter in the mammalian central nervous system and neuronal pathways in the brain which is related to several neurological disorders, such as schizophrenia, Parkinson's disease, epilepsy and stroke [1-3].

Glutamate dehydrogenase (GD) is an enzyme presents in most microbes and the mitochondria of eukaryotes, as a required enzyme for urea synthesis. GD converts glutamate to α -Ketoglutarate and vice versa (Fig. 1). NAD^+ is a cofactor for the glutamate dehydrogenase reaction, producing α -Ketoglutarate and ammonium as a byproduct. The isoelectric point (Ip) of GD is about $\text{pH}=4.83$, therefore, at $\text{pH} > \text{Ip}$, it is net negatively charged, while at $\text{pH} < \text{Ip}$, it is positively charged.

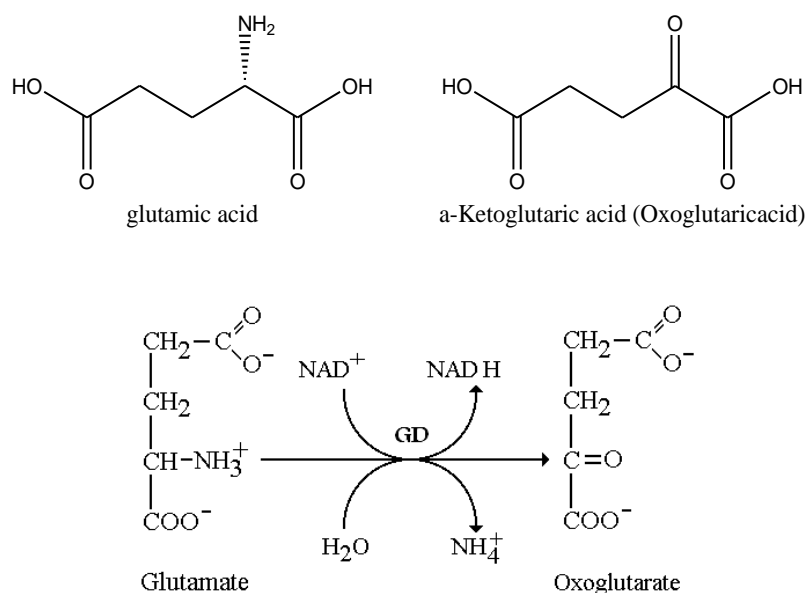


Figure 1. Chemical Structure of glutamic acid and α -Ketoglutaric acid and glutamate dehydrogenase reaction

Metal nanoparticles have generally high effective surface area, catalysis and biocompatibility properties [4-11]. One of their important functions is catalytic activity. This property is more remarkable in noble metal nanoparticles. Because metal nano particles also have good biocompatibility, they are extensively used to immobilize biomolecules in construction of biosensor. Pt nanoparticles have been widely applied in biosensors due to their excellent catalytic action.

Multiwall carbon nanotubes (MWCNTs) have been recently used in construction of biosensors due to their high surface area, high surface/volume ratio, good electrical conductivity and significant mechanical strength [11-20]. Nafion, due to its easy fabrication, good electrical conductivity, high chemical stability and good biocompatibility, has been widely used as a protective coating material and as a support for enzyme immobilization [21].

This work introduces a new flow injection electrochemical biosensor combine with FFT continuous cyclic voltammetry (FFTCCV) technique [22-27] as a sensitive method for rapid determination of glutamate (Fig. 1). To the best of our knowledge, this is the first application of

FFTCCV method for glutamate biosensor based on glutamate dehydrogenase (GD) immobilized on MWCNT/Pt nanoparticle. In addition, the fabrication, characterization and analytical performance of the biosensor were investigated. The experimental parameters, which can affect the sensor performance, were optimized and the electrochemical characteristics of the sensor were described.

2. MATERIALS AND METHODS

2.1. Reagents

All chemicals and solvents used were of analytical grade and were used as received. Glutamate dehydrogenase (GD, EC 1.4.1.3, MW 300,000, from bovine liver, suspension in 2.0 M $(\text{NH}_4)_2\text{SO}_4$ solution, 48 units/mg), l-glutamate (monosodium salt, 99%), dihydrogen platinum tetrachloride (H_2PtCl_4), nafion (5 % wt.) solution in a mixture of lower aliphatic alcohols and water and β -nicotinamide adenine dinucleotide (NAD^+) were purchased from Sigma–Aldrich. MWCNTs (diameter: 10–20 nm; length: 0.5–40 nm; purity: $\geq 95\%$) were obtained from Shenzhen Nanotech Port Ltd. Co (Shengzhen, China). Phosphate buffer solutions (PBS, 0.1 M) with various pH values were prepared by mixing stock standard solutions of K_2HPO_4 and KH_2PO_4 and adjusting the pH with H_3PO_4 or NaOH. All solutions were made up with doubly distilled water.

2.2. Preparation of glutamate biosensor

PtNPs were electrochemically deposited on the cleaned surface of GCE (0.4 mm^2) with constant potential at -0.25V for a short time in a 5-mL solution containing 1 mM H_2PtCl_4 and 0.5 M H_2SO_4 . After the deposition, the electrode was thoroughly rinsed with water and allowed to dry at room temperature to form a thin NPs-layer. After this procedure, 5 μL solution of glutamate dehydrogenase and MWCNTs (2–10 mg/mL) (in phosphate buffer solution (PBS) pH=7.2 and 0.9% NaCl) was coated on the PtNPs, and dried at room temperature for 10 min to form a biocatalytical enzyme layer. The electrode is kept overnight for enzymes immobilization and then washed with buffer solution. After drying the modified GD-MWNT/PtNPs/GC electrode (see Fig. 2), a 10.0 μL nafion solution was dropped onto the electrode and dried for 12 h at $4.0 \text{ }^\circ\text{C}$ to form a film on the modified electrode. When, not in use, the modified GC electrodes were stored in PBS at $4.0 \text{ }^\circ\text{C}$.

2.3. Instrumentation

For the electrochemical FFTCCV experiments a homemade potentiostat was used. The measurement system was controlled by a PC PIV for acquiring and storing the data. For the measurements, electrochemical software was developed using Delphi 6.0. In this system, generating the analog waveform and acquiring current was controlled by an analog to digital (A/D) data acquisition board (PCL-818H, Advantech Co.). During the experiment, the potential waveform was

repeatedly applied to the biosensor. Moreover, in this detection setup, the data were processed and plotted in real time, and stored, and then the data could be loaded and plotted the voltammograms.

2.4. Flow Injection Setup

All of the flow injection analysis use for measurements [28], the equipment was integrated with an eight roller peristaltic pump (UltrateckLabs Co., Iran) and a four way injection valve (Supelco Rheodyne Model 5020) with 900 μL sample injection loop. The analyte solutions were introduced into the sample loop by means of a plastic syringe. The electrochemical cell used in flow injection analysis is shown in Fig. 2.

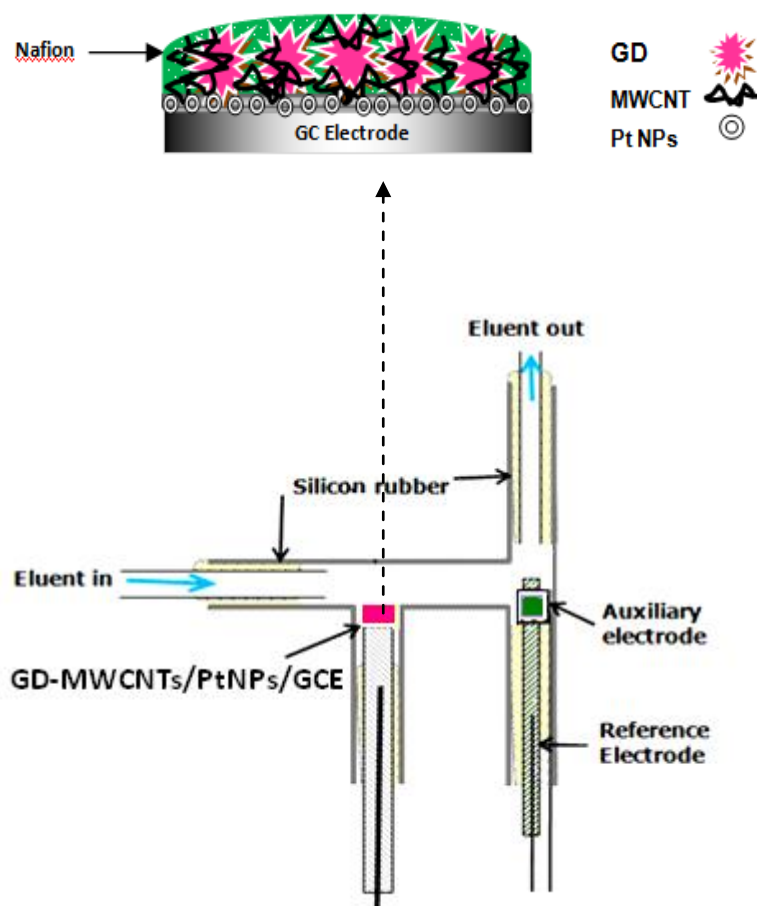


Figure 2. The diagram of GD-MWCNT/PtNPs/GC biosensor and the electrochemical cell used in flow injection analysis

The used eluent in the flow injection measurements is NAD^+ (1.0 mM) in the PBS (pH=7.2). The glutamate biosensor described in this work is based on the oxidation of L-glutamate by NAD^+

through catalytic activity of glutamate dehydrogenase (GD). Reduction of NAD^+ to NADH on the modified surface of the electrode leads to produce an electrochemical signal.

3. RESULTS AND DISCUSSION

The surface area of the biosensor electrode and the sensitivity of the FFTCV method can be influenced by physical morphology of the electrode. Therefore, the electrode was characterized using scanning electron microscopy (SEM) [29] and Electrical impedance spectroscopy (EIS) [30]. Fig. 3 shows the typical SEM image of GD-MWCNT/PtNPs/GC electrode surface in which the film was formed as bright round-shaped, homogeneously dispersed and shows an obvious formation of composite film.

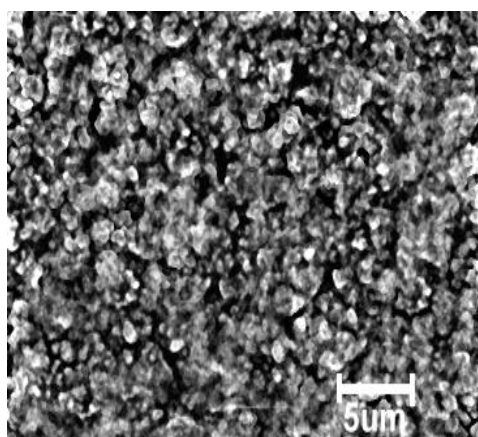


Figure 3. SEM image of the electrode GD-MWCNT/PtNPs/GCE

Fig. 4 illustrates the results of EIS on bare GCE (curve 1), PtNPs/GCE (curve 2) GD-MWCNT/PtNPs/GC (curve 3) in the presence of equivalent 15 mM $\text{Fe}(\text{CN})_6^{4-/3-}$ and 0.1 M KCl, which are measured at the formal potential of $\text{Fe}(\text{CN})_6^{4-/3-}$. Fig. 4 shows a semicircle of about 900 Ω for the bare GCE, which indicates a low electron transfer resistance to the redox-probe in the electrolyte solution. The diameter of the high frequency semicircle was obviously reduce to less than 500 Ω by the surface modification by PtNPs layer, suggesting that a significant acceleration of the $\text{Fe}(\text{CN})_6^{4-/3-}$ redox reaction occurred. Also, the further deposition of GD-MWCNT/PtNPs layer cause the resistance of the high frequency semicircle (760 Ω) increased (curve 3), which indicates a higher resistance to the anion redox reaction at GD-MWCNT/PtNPs/GCE. This may be attributed to the lesser conductivity of the surface deposited nafion/GD.

The Randles circuit (inset in Fig. 4) is chosen to fit the obtained impedance data containing the electron transfer process. The equivalent circuit was considered in order to analyze the impedance spectroscopy data. The first resistance is related to the electrical behavior of the solution. The capacitor

C_d models the double-layer, the resistance R_2 is related to charge transfer, Z_w is the Warburg impedance related to the ion transfer phenomenon. The constant phase element (CPE) is used for the diffusion at low frequencies. The last constant phase element is modeling the low frequency behavior of the cell.

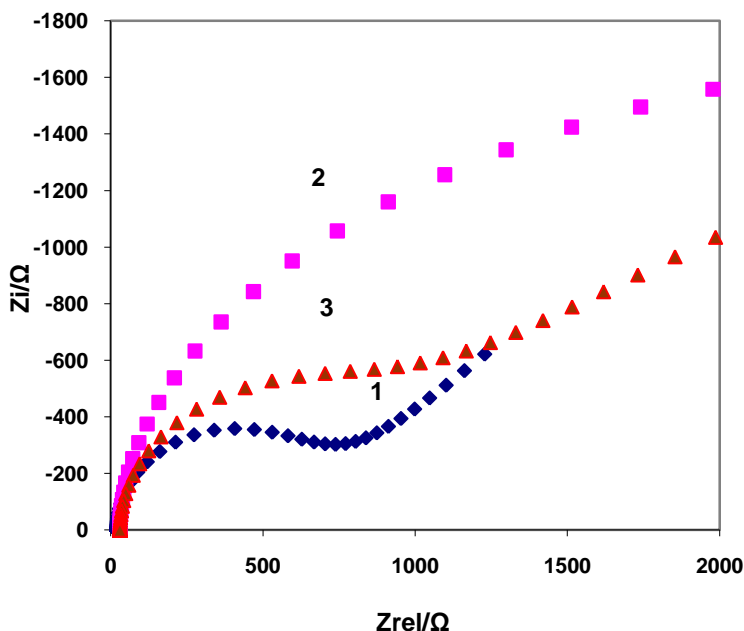


Figure 4. EIS plots in 15 mM $K_3[Fe(CN)_6]/K_4[Fe(CN)_6]$ (1:1) mixture containing 0.1 M KCl at bare GCE (1) PtNPs/GCE (2) and GD-MWCNT/PtNPs/GCE (3), respectively; Inset is three elements cell equivalent circuit for the linear diffusion impedance.

The prepared GD-MWCNT/PtNPs/GC was first activated in NAD^+ (1.0 mM) in PBS (pH 7.2) by FFTCCV scans from -100 mV to 1000 mV until stable baseline curve was obtained. In the measurements a FIA system was design and 900 μ L of various concentrations of glutamate were injected into the cell. Fig. 5a demonstrates typical differentiated FFTCCVs of the GD-MWCNT/PtNPs/GC electrode in the potential range of -100 to 1000 mV at potential sweep rate 5 Vs^{-1} . In the Figure, the time axis represents the time passing between the beginning of the flow injection experiment and the beginning of sweeps (i.e. it represents a quantity proportional to the sweep number) [14-21]. Also, the figure shows that before injection (in absent of analyte) there is no significant changes, but by injection of 900 μ L of 3.0×10^{-6} M glutamate in 0.3 mM buffer solution (PBS) at pH=7.2 a signal appears at potential 850 mV. Before injection of the analyte, GD-MWCNT/PtNPs/GC electrode in NAD^+ (1.0 mM) and 1.0 mM PBS showed small peaks that are related to oxidation and reduction of PtNPs in the film. However, after background subtraction the net current changes are appears in the CVs. These current changes are shown in Fig. 5B in two dimensional forms.

In fact, this peak came from the reduction of NAD^+ to NADH, which is catalyzed by the immobilized GD. Also, the presence of GD-MWCNT/PtNPs/GC at electrode surface possesses a

natural conductive property and catalytic behavior, which can provide a good conductive pathway to the electron transfer of via the redox center of the enzyme.

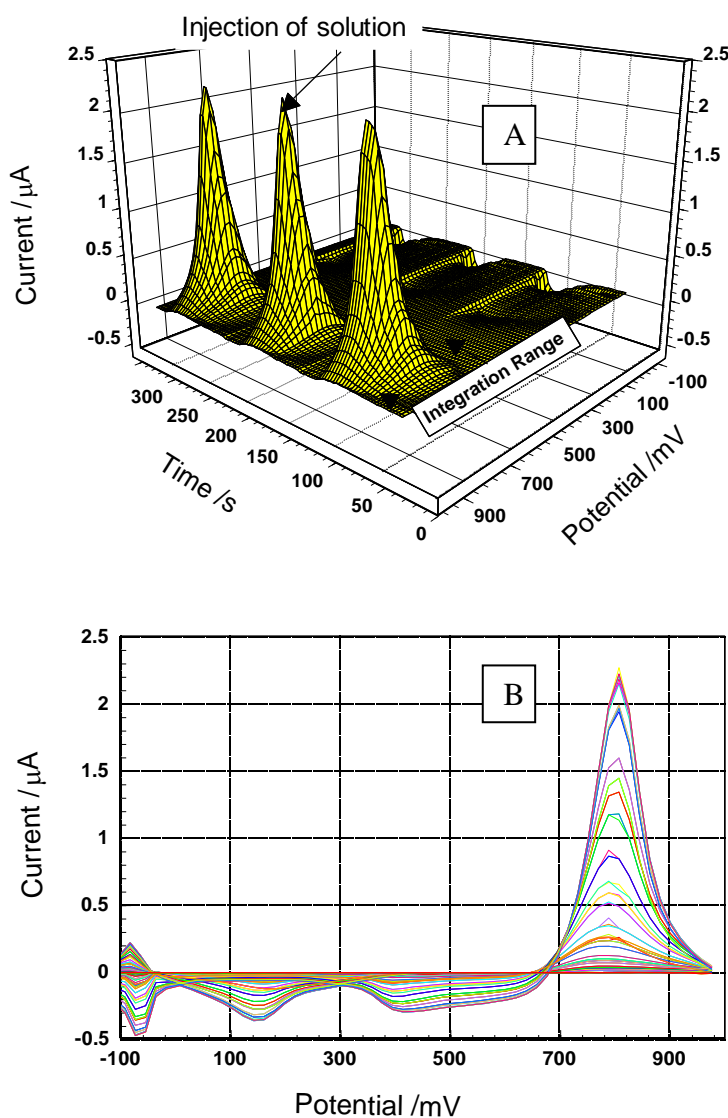


Figure 5. A) Differentiate (background subtracted) form of the recorded FFT cyclic voltammograms of the GD-MWCNT/PtNPs/GC electrode without (in absent) and with injection of 900 μL of 4.0×10^{-6} M glutamate in 1.0 mM PBS at pH=7. 2 in the potential range of -100 to 1000 mV at 5 V/s. B) Two dimensional of the graph A

According to Fig. 1, the electrochemical reaction for the detection of glutamate in presence of GD is a catalyst reaction. When FFTCCV is used to monitor a flowing system, glutamate electrochemical processes will cause a measurable change in the peak current at the voltammograms and the data processing operation is carried out simultaneously with data acquisition during flow injection experiments. The response was calculated as;

$$\Delta Q = Q - Q_0 \quad (1)$$

where ΔQ is the electrical charge obtained by integration of currents between 700 and 1000 mV, and Q_0 represents Q in the absence of the adsorbent. This integration range for the current is shown in Fig. 5. In this method, ΔQ is calculated based on the all-current changes at the CV. A total absolute difference function (ΔQ) can be calculated by using the following equation:

$$\Delta Q (s\tau) = \Delta t \left[\sum_{E=E_i}^{E=E_f} |i(s, E) - i(s_r, E)| \right] \quad (2)$$

Where, s is the sweep number, τ is the time period between subsequent potential scan, Δt is the time difference between two subsequent points on the cyclic voltammograms, $i(s, E)$ represents the current of the cyclic voltammograms recorded during the s -th scan and $i(s_r, E)$ is the reference current of the cyclic voltammograms. E_i and E_f are the initial and the final potential, respectively, for integrating of the currents. The results show that with increasing the concentration of glutamate in the injected sample, ΔQ increases. However, in order to reach to maximum sensitivity, it is needed the important factors that have influence on the detection system to optimize.

3.1. Optimizing the experimental parameters

Fig. 6 presents the influence of the scan rates and the eluent flow rate on the sensitivity of the biosensor response, at scan rates (from 0.5 to 10 V/s) and the eluent flow rate (0.2 to 4 mL min⁻¹) from injecting solutions of 3.0×10^{-6} M of glutamate. In fact, the measurement method, sensitivity of the biosensor depends on the potential sweep rate and eluent flow rate.

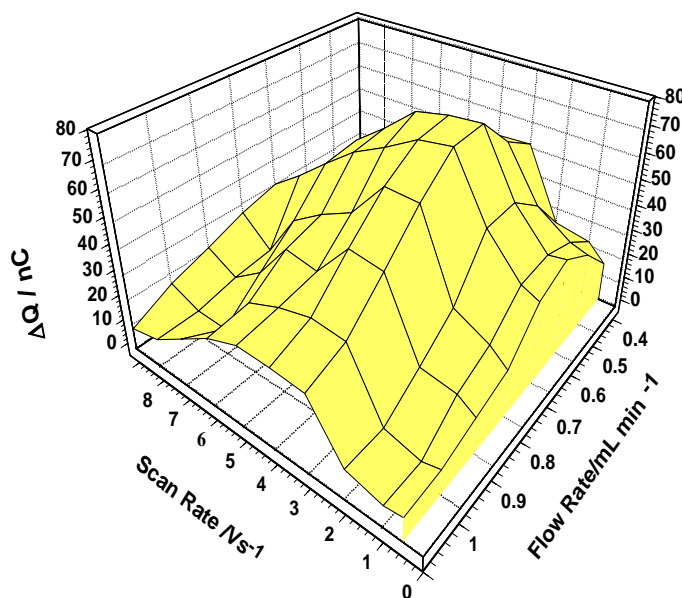


Figure 6. Effect of the sweep rate and effect of flow rate on the response of the biosensor

As it is shown in Fig. 6, the biosensor demonstrates the maximum sensitivity (or signal) at 5 V/s of scan rate and 0.7 mL min^{-1} of the eluent flow rate. This is mainly due to kinetic factors of the electrode processes, and instrumental limitations [31-40]. Nevertheless, the effects of the sweep rate on the biosensor performance can be taken into consideration from three different parameters; speed of data acquisition, kinetic factors of electrochemical processes at the electrode surface, and the flow rate of the eluent. The main reason for lower sensitivity of the biosensor at higher scan rates is limitation in the electron transfer rate of electrochemical processes of glutamate with the biosensor.

3.2. Effect of pH, PtNPs, MWCNT, GD and temperature on the biosensor

Investigation of the effect of the pH value on the performance of the biosensor is very importance, because the activity of the immobilized GD is pH dependent. The results of measurements of the electrode response ΔQ in the pH range 5.0–8.0 (see Fig. 7), indicate that ΔQ response realizes to maximum at pH 7.2, where the activity of the enzyme is the highest.

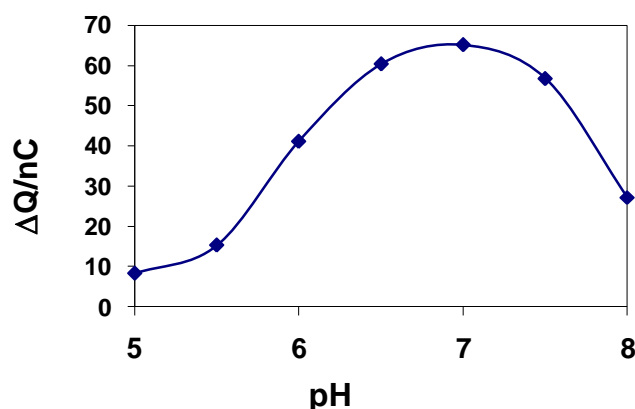


Figure 7. The effect of pH on response of the biosensor to $4.0 \times 10^{-6} \text{ M}$ glutamate in 1.0 mM PBS at pH=7. 2

Fig. 8 shows the effect of amount of PtNPs and MWCNTs on GD/MWCNT/PtNPs/GC electrode after injections of $4.0 \times 10^{-6} \text{ M}$ glutamate in 1.0 mM PBS at pH=7. 2. As shown, the value of ΔQ increases with increasing the time of the deposition of PtNPs and reaches to a maximum around 25s. On the other hand, at higher deposition time the value of ΔQ decrease. Also, Fig. 8 shows the change of the biosensor sensitivity with the amount of MWCNTs added to the content of the electrode surface. The graph indicates that the value of ΔQ increase with the adding volume of MWCNTs and then reaches s to a constant value. Fig. 9A shows the change of the biosensor sensitivity with the amount of GD added to the content of the electrode surface. The graph indicates that the value of ΔQ increase with the adding volume of GD and then reaches to a constant value. It is appears that more than $6.0 \mu\text{L}$ GD the electrode goes to a saturation state. Fig. 9b the influence of temperature on the biosensor response was also investigated. The electrode was immersed into the eluent solution at a given temperature. As shown in Fig. 9B, the ΔQ increases with increasing temperature from 10 to 33

°C and then decreases as the temperature increased. Although the response was greatest at 33 °C, for practical reasons it was suggested that room temperature be used to prolong the useful lifetime of the biosensor, because in the most enzymes they can be easily denatured at high temperature.

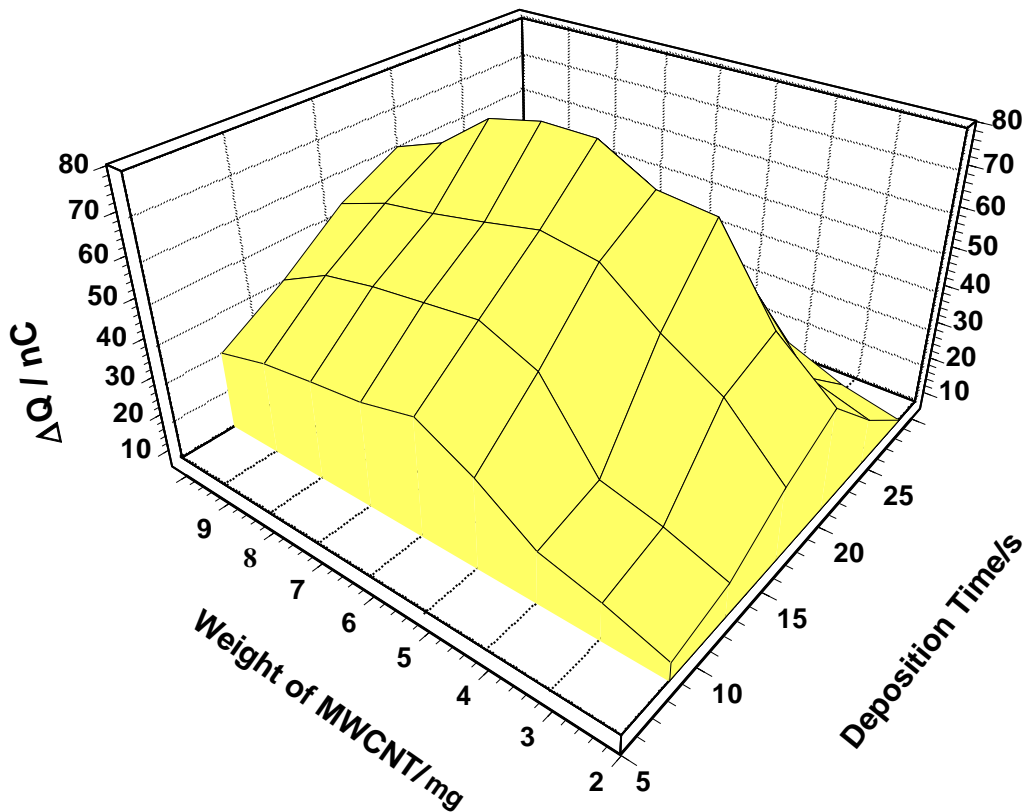


Figure 8. The effect of deposition time of Pt NPs and MWCNT weight on response of the biosensor to 4.0×10^{-6} M glutamate in 1.0 mM PBS at pH=7. 2

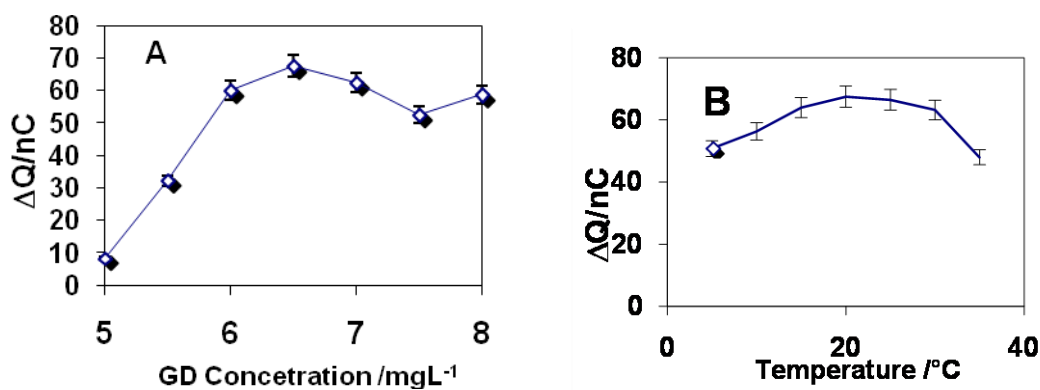


Figure 9. A)The effect of GD concentration and B) influence of temperature on response of the biosensor of 4.0×10^{-6} M glutamate in 1.0 mM PBS at pH=7. 2

3.3. Calibration curve and biosensor characterization

The inset of Fig. 10 shows the typical FFTCCV responses of GD-MWCNT/PtNPs/GC bioelectrodes for the successive injection glutamate solution. The ΔQ responses of the biosensor were obtained for standard solutions of glutamate from 0.1 to 400 μM in 1.0 mM PBS at pH 7.2 solution. The point in the calibration curve represent the integrated currents for 3 to 5 consecutive flow injections of the standard solution in FFTCCV flow injection method.

Following linear regression analysis [40-46], the linearity was evaluated by linear regression analysis, which calculated by the least square regression method, and the correlation coefficient of $R=0.9926$ with %R.S.D. were obtained from 0.24 to 3% in the concentration range 0.1 to 10 μM .

The detection limit, estimated based on signal to noise ratio ($S/N=3$), was found to be 30 ± 0.2 nM. The long-term storage stability of the sensor was tested for 44 days. The sensitivity retained 92.3% of initial sensitivity up to 60 days which gradually decreases, gradually by the time of usage, might be due to the loss of the catalytic activity of the enzyme.

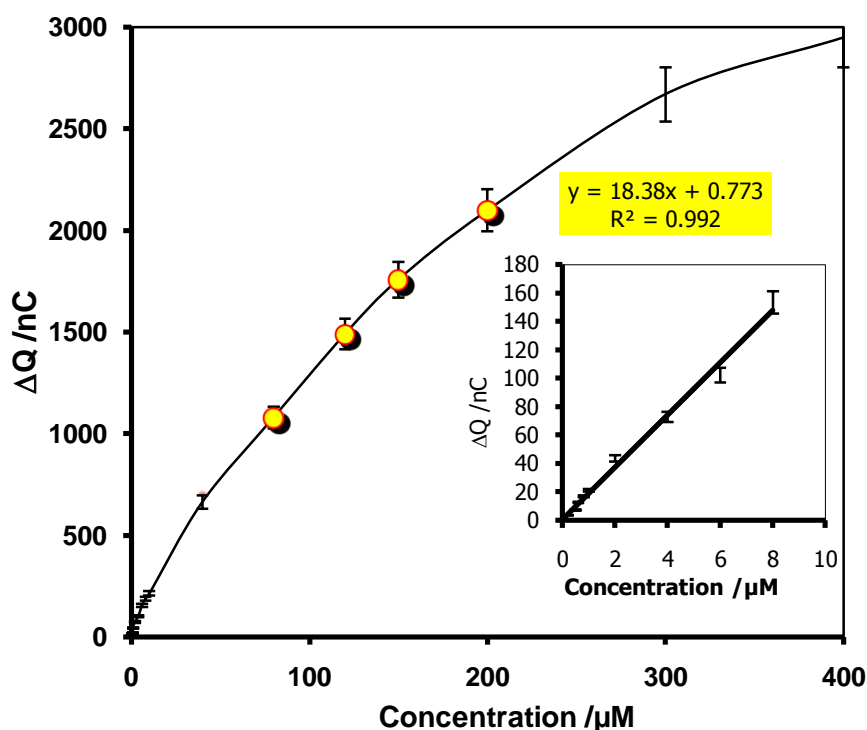


Figure 10. The calibration curve for glutamate determination in 1.0 mM PBS at pH=7.2 in FIA measurements

4. CONCLUSIONS

In this work, GD-MWCNT/PtNPs/GC biosensor is introduced for determination of glutamate in flow injection analysis system. The biosensor is constructed by modifying the GC electrode surface

with GD-MWCNTs, and based on the inherent conductive properties of PtNPs. The present results showed that the electrode in flowing solution exhibited a higher affinity to its substrate and produced detectable and fast response in FFTCCV method in FIA measurement. To the best of our knowledge, the method is the first time that a very high-sensitivity and low detection FIA that is used for glutamate. In addition, it was realized that the biosensor had an excellent producible sensitivity of $4 \mu\text{CnM}/\text{cm}^{-2}$, response time less than 18 s for the glutamate solution.

References

1. C. Xue, Y. Li and M.E. Wolf, *J. Neurochem.* 67 (1996) 352.
2. R.L. Villarta, D.D. Cunningham and G.G. Guilbault, *Talanta* 38 (1991) 49.
3. M.E. Wolf, *Prog. Neurobiol.* 54 (1998) 679.
4. M. R. Nabid, M. Golbabaee, A. B. Moghaddam, R. Dinarvand and R. Sedghi, *Int. J. Electrochem. Sci.* 3 (2008), 1117.
5. Y. F. Zhang, G. P. Guo, F. Q. Zhao, Z. R. Mo, F. Xiao, and B. Z. Zeng, *Electroanalysis* 22 (2010) 223.
6. L. Zhang, Z. Fang, G. C. Zhao and X. W. Wei, *Int. J. Electrochem. Sci.*, 3 (2008) 746.
7. N. German, A. Ramanaviciene, J. Voronovic, and A. Ramanavicius, *Microchim. Acta* 168 (2010) 221.
8. A. B. Moghaddam, T. Nazari, J. Badraghi and M. Kazemzad, *Int. J. Electrochem. Sci.* 4 (2009), 247.
9. Y. Zhang, P. He and N. Hu, *Electrochim. Acta* 49 (2004) 1981.
10. J. P. Singh, X. G. Zhang, H. L. Li, A. Singh and R. N. Singh, *Int. J. Electrochem. Sci.*, 3 (2008) 416.
11. J. S. Xu and G. C. Zhao, *Int. J. Electrochem. Sci.*, 3 (2008) 519.
12. P. M. Ajayan, *Chem. Rev.* 99 (1999) 1787.
13. G. P. Keeley and M. E. G. Lyons, *Int. J. Electrochem. Sci.*, 4 (2009) 794.
14. A. Mohammadi, A. B. Moghaddam, R. Dinarvand and S. Rezaei-Zarchi, *Int. J. Electrochem. Sci.*, 4 (2009) 895.
15. J. Zhong, L. Song, J. Meng, B. Gao, W.S. Chu, H.Y. Xu, Y. Luo, J.H. Guo, A. Marcelli, S.S. Xie and Z.Y. Wu, *Carbon* 47 (2009) 967.
16. H. J. Wang, C. M. Zhou, J. H. Liang, H. Yu and F. Peng, *Int. J. Electrochem. Sci.*, 3 (2008) 1180.
17. H. Yaghoobian, H. Karimi-Maleh, M. A. Khalilzadeh and F. Karimi, *Int. J. Electrochem. Sci.*, 4 (2009) 993.
18. H. R. Zare, R. Samimi and M. M. Ardakani, *Int. J. Electrochem. Sci.*, 4 (2009) 730.
19. H. R. Zare and N. Nasirizadeh, *Int. J. Electrochem. Sci.*, 4 (2009) 1691.
20. L. Q. Liu, F. Q. Zhao, F. Xiao and B. Z. Zeng, *Int. J. Electrochem. Sci.*, 4 (2009) 525.
21. L. Zhang, Z. Fang, Y. H. Ni and G. C. Zhao, *Int. J. Electrochem. Sci.*, 4 (2009) 407.
22. P. Norouzi, M. R. Ganjali, B. Larijani, A. Mirabi-Semnakolaii, F. S. Mirnaghi, and A. Mohammadi, *Pharmazie* 63 (2008) 633.
23. P. Norouzi, H. Rashedi, T. Mirzaei Garakani, R. Mirshafian and M. R. Ganjali, *Int. J. Electrochem. Sci.* 5 (2010) 377.
24. P. Daneshgar, P. Norouzi, F. Dousty, M. R. Ganjali, and A. A. Moosavi-Movahedi, *Curr. Pharm. Anal.* 5 (2009) 246.
25. P. Norouzi, M. R. Ganjali, S. Shirvani-Arani, and A. Mohammadi, *J. Pharm. Sci.* 95 (2007) 893.
26. M. R. Pourjavid, P. Norouzi, and M. R. Ganjali, *Int. J. Electrochem. Sci.* 4 (2009) 923.
27. P. Norouzi, M. R. Ganjali, M. Zare, and A. Mohammadi, *J. Pharm. Sci.* 96 (2007) 2009.
28. P. Norouzi, M. Qomi, A. Nemati, and M. R. Ganjali, *Int. J. Electrochem. Sci.* 4 (2009) 1248.

29. P. Daneshgar, P. Norouzi, M. R. Ganjali and F. Dousty, *Int. J. Electrochem. Sci.*, 4 (2009), 444.
30. A. Mohammadi, A. B. Moghaddam, R. Dinarvand, J. Badraghi, F. Atyabi and A. A. Saboury, *Int. J. Electrochem. Sci.*, 3 (2008) 1248.
31. M. Ates, *Int. J. Electrochem. Sci.*, 4 (2009) 980.
32. P. Norouzi, B. Larijani, M. Ezoddin and M. R. Ganjali, *Mater. Sci. Eng. C* 28 (2008) 87.
33. M. R. Ganjali, P. Norouzi, R. Dinarvand, R. Farrokhi, and A. A. Moosavi-Movahedi, *Mater. Sci. Eng. C* 28 (2008) 1311.
34. D. Du, S. Chen, J. Cai, and A. Zhang, *Biosens. Bioelectron.*, 23 (2007) 130.
35. L. Liua, Z. Yina and Z. Yang, *Bioelectrochemistry*, 79 (2010) 84.
36. M. E.G. Lyons, and G. P. Keeley, *Int. J. Electrochem. Sci.*, 3 (2008) 819.
37. H.J. Wang, C.M. Zhou, F. Peng, and H. Yu, *Int. J. Electrochem. Sci.*, 3 (2008) 1258.
38. P. Norouzi, F. Faridbod, B. Larijani, M. R. Ganjali, *Int. J. Electrochem. Sci.*, 5 (2010) 1213.
39. P. Norouzi, M. Pirali-Hamedani, F. Faridbod, M. R. Ganjali, *Int. J. Electrochem. Sci.*, 5 (2010) 1225.
40. P. Norouzi, M. R. Ganjali, and L. Hajiaghababaei, *Anal. Lett.*, 39 (2006) 1941.
41. P. Norouzi, G. R. Nabi Bidhendi, M.R. Ganjali, A. Sepehri, M. Ghorbani, *Microchim. Acta*, 152 (2005) 123.
42. P. Norouzi, M. R. Ganjali, T. Alizadeh, and P. Daneshgar, *Electroanalysis*, 18 (2006) 947.
43. M. R. Ganjali, P. Norouzi, M. Ghorbani, and A. Sepehri, *Talanta*, 66 (2005) 1225.
44. M. R. Ganjali, P. Norouzi, S. Shirvani-Arani, and A. Mohammadi, *Russian J. Electrochem.* 44 (2008) 158.
45. M. R. Ganjali, P. Norouzi, and M. Zare, *Russian J. Electrochem.* 44 (2008) 1135.
46. P. Norouzi, F. Faridbod, E. Nasli-Esfahani, B. Larijani, M. R. Ganjali, *Int. J. Electrochem. Sci.*, 5 (2010) 1008.